Chapter 3: Research and calculations for DCS development

3.1 Introduction

In Chapter 2, the limitations, problems and challenges pertaining to the mine's compressed air system were underlined. From this, a user requirement for the DCS was formulated.

The research and calculations required for the development of the DCS is presented in this chapter. The concluding paragraph of this chapter offers a solution for the DCS.

This study will be restricted to one-dimensional incompressible fluid flow. Fluid flow measurement, pipe friction losses and compressed air network properties are applied to ensure optimum compressor selection.

The following assumptions are made for the calculations:

- The flow of the compressed air network is at a steady state, one-dimensional, fully developed and isothermal.
- Pipe roughness is constant over the entire compressed air network.
- Historical data is correct.

3.2 Fluid properties

The average inlet and exit temperatures of the compressors were calculated from logged historical data as 299 K (25℃) and 316 K (43℃) respectively. The exit temperature will be used for isothermal flow calculations, an assumption made by other researchers [22, p. 2254], [23, p. 171]. Pressure meters are installed at each shaft entrance and at the compressor house exit and are accurate to within 0.15% [24].

3.2.1 Heat index and gas constant of air

For this application, Engineering Equation Solver (EES)[4] was used to calculate the difference between the minimum and maximum values of the heat index and the gas constant respectively. The error made by assuming these values to be constant amounted to less than 1%. The Adiabatic Heat Index, n, of 1.4 and gas constant, R, for air equal to 287 J/kg-K, was used in the calculations.

3.2.2 Density of air

The density of compressed air, ρ [kg/m^3], changes considerably as the pressure varies, as shown in Figure 16.

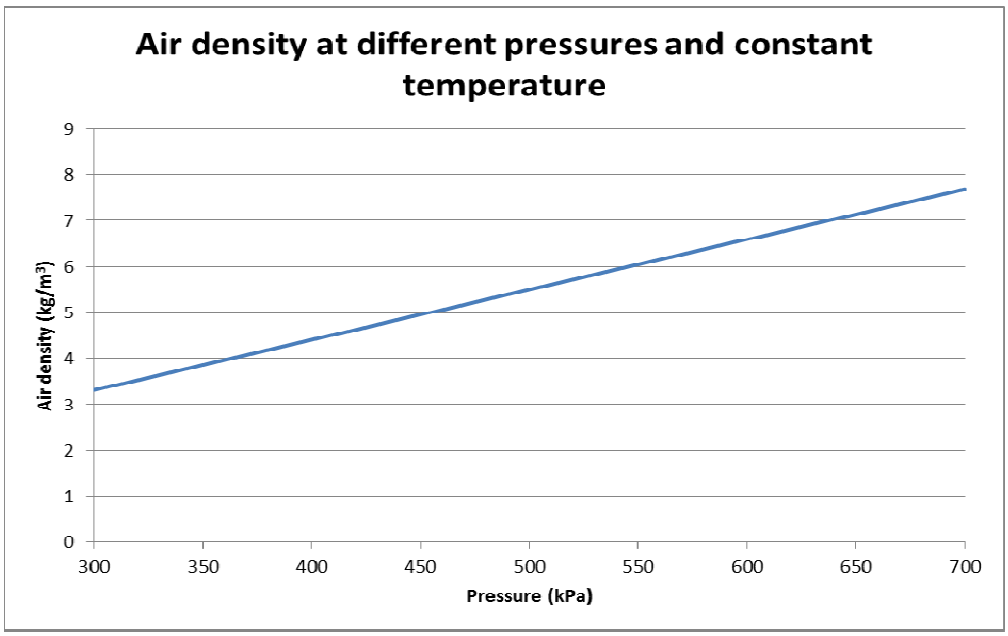

Figure 16: Air density at different pressures

[4] EES developed by F-Chart Software, http://www.fchart.com/ees/.

For the pressure range shown, there is a difference of approximately 40%. Therefore, the air density is calculated during each simulation iteration.

3.2.3 Viscosity of air

The viscosity of a fluid, μ [kg/m-s], is the resistance to relative motion [25, p. 246], [26, p. 1]. At 316 K, the viscosity varies by less than 0.1 % for a pressure range of 300 kPa to 700 kPa. The average viscosity for this pressure range, 3,0134 x 10^{-5} kg/m-s, was used.

3.2.4 Reynolds number

The Reynolds number is a dimensionless value used in fluid mechanics calculations to distinguish between laminar and turbulent flow [27, p. 363], [28, p. 2].

$$\mathrm{Re} = \frac{\rho V D}{\mu} \qquad 3.1$$

Where ρ is the density;
v is the fluid velocity;
D is the pipe diameter; and
μ is the viscosity.

Even though the Reynolds number for this application is always large enough to ensure turbulent flow, it was calculated for each iteration to determine the pipe friction loss factor.

3.3 Bernoulli's Theorem

Bernoulli's Theorem can be used for a frictionless, incompressible fluid along a streamline [27, p. 128]. Equation 3.2 shows Bernoulli's Equation [29, p. 336], [27, p. 100].

$$\frac{\rho v^2}{2} + \rho g z + P = \text{constant} \tag{3.2}$$

where ρ is the fluid density;
v is the fluid velocity;
g is gravitational acceleration; and
z is the height measured from an arbitrary datum line.

Equation 3.3 shows Bernoulli's Equation applied between any two points in a streamline [27, p. 112].

$$\frac{\rho_1 v_1^2}{2} + \rho_1 g z_1 + P_1 = \frac{\rho_2 v_2^2}{2} + \rho_2 g z_2 + P_2 \tag{3.3}$$

An approximate constant height across the compressed air network on the surface is assumed. The actual change in altitude does not exceed 1%. Bernoulli's Equation can then be written as:

$$\frac{\rho_1 v_1^2}{2} + P_1 = \frac{\rho_2 v_2^2}{2} + P_2 \tag{3.4}$$

However, frictional losses were included in this study. Bernoulli's Equation can then be written as [27, p. 416]:

$$\frac{\rho_1 v_1^2}{2} + P_1 = \frac{\rho_2 v_2^2}{2} + P_2 + P_{loss} \quad 3.5$$

where P_{loss} is the pipe friction losses between the two points under consideration.

Equations 3.2, 3.3 and 3.5 are applicable to incompressible fluids [27, p. 128]. Equation 3.6 shows Bernoulli's Equation for frictionless compressible flow [27, p. 129].

$$\frac{\rho_1 v_1^2}{2} + \left(\frac{n}{n-1}\right) P_1 = \frac{\rho_2 v_2^2}{2} + \left(\frac{n}{n-1}\right) P_2 \quad 3.6$$

with n the heat index of air.

For a Mach number of approximately 0.3, the compressible and incompressible fluid equations differ by about 2% [27, p. 130]. Figure 17 on the following page shows the pressure ratio as defined by Munson et al. as a function of Mach number for frictionless incompressible and compressible flow, Equation 3.4 and Equation 3.6 respectively.

For the conditions encountered in this study, the flows in the pipes will rarely exceed Mach 0.3 and incompressible flow will be assumed for the compressed air network.

A diffuser makes use of Bernoulli's Principle to reduce the air flow and convert kinetic energy into pressure energy. Figure 18 shows an example of a diffuser after a compressor stage at the compressor outlet.

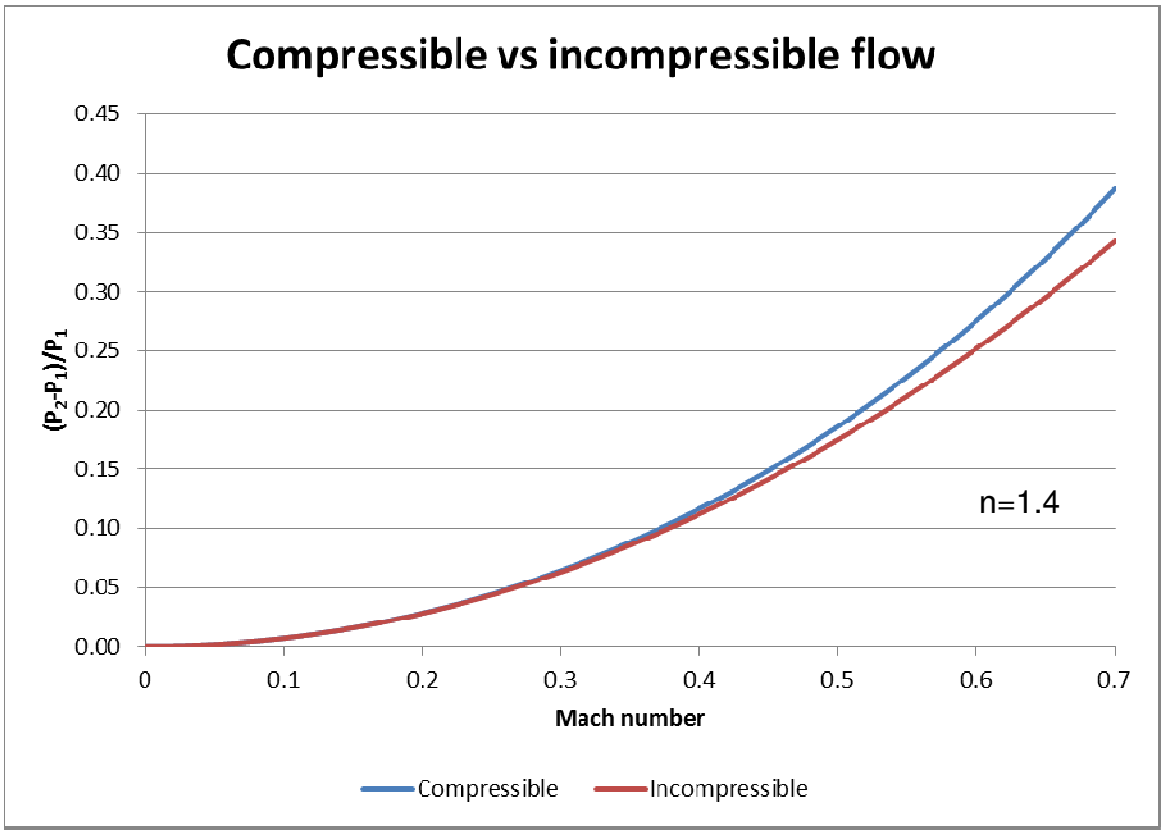

Figure 17: Pressure ratio as a function of Mach number [27, p. 130]

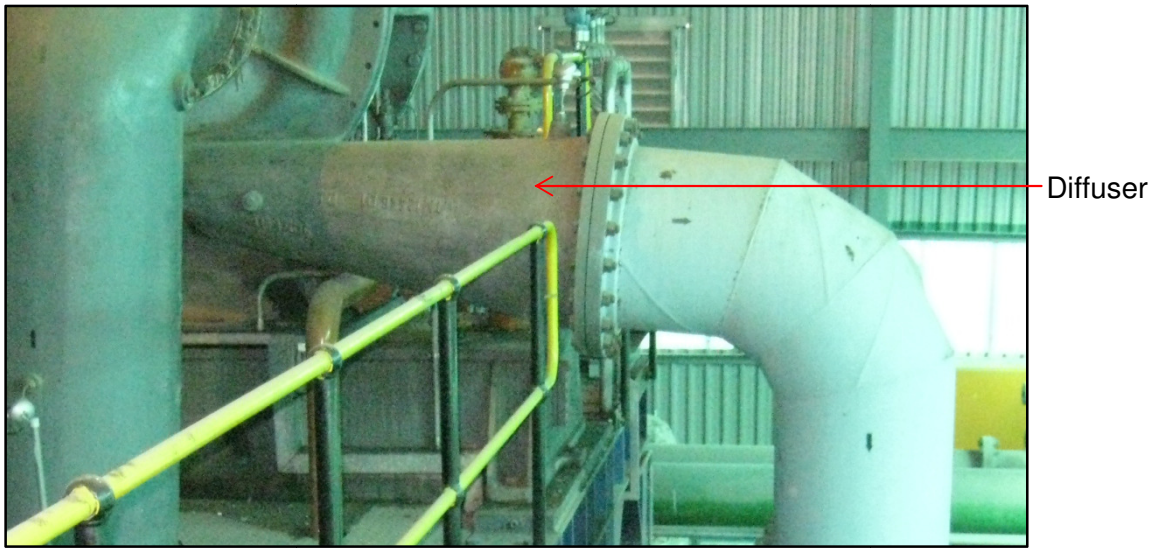

Figure 18: Compressor diffuser

3.4 Conservation of mass and the mass flow of air

The mass flow Equation 3.7 is [27, p. 115]:

$$\dot{m} = \rho v A = \rho Q \qquad 3.7$$

where ρ is the density;
v is the average fluid velocity;
Q is the volume flow; and
A is the internal cross-section area of the pipe.

Consider a fixed control volume for a compressed air network. The principle of conservation of mass, shown in Equation 3.8, can be applied to derive the continuity equation for steady fluid flow [30, p. 168], shown in Equation 3.9 [27, p. 115]:

$$\dot{m}_{in} = \dot{m}_{out} \qquad 3.8$$

$$\rho_1 v_1 A_1 = \rho_2 v_2 A_2 \qquad 3.9$$

In practice, pipe leaks occur and therefore the mass flow into a specific section of the compressed air network will probably be greater than the exit mass flow. For the DCS calculations, losses due to leaks were assumed to be negligible.

Flows are measured at the shafts using permanently installed flow meters that have a maximum error of 0.5% for low flows. In the 50 to 100% calibrated flow range, the error is as small as 0.1% [31]. Figure 19 illustrates a typical flow meter at the mine.

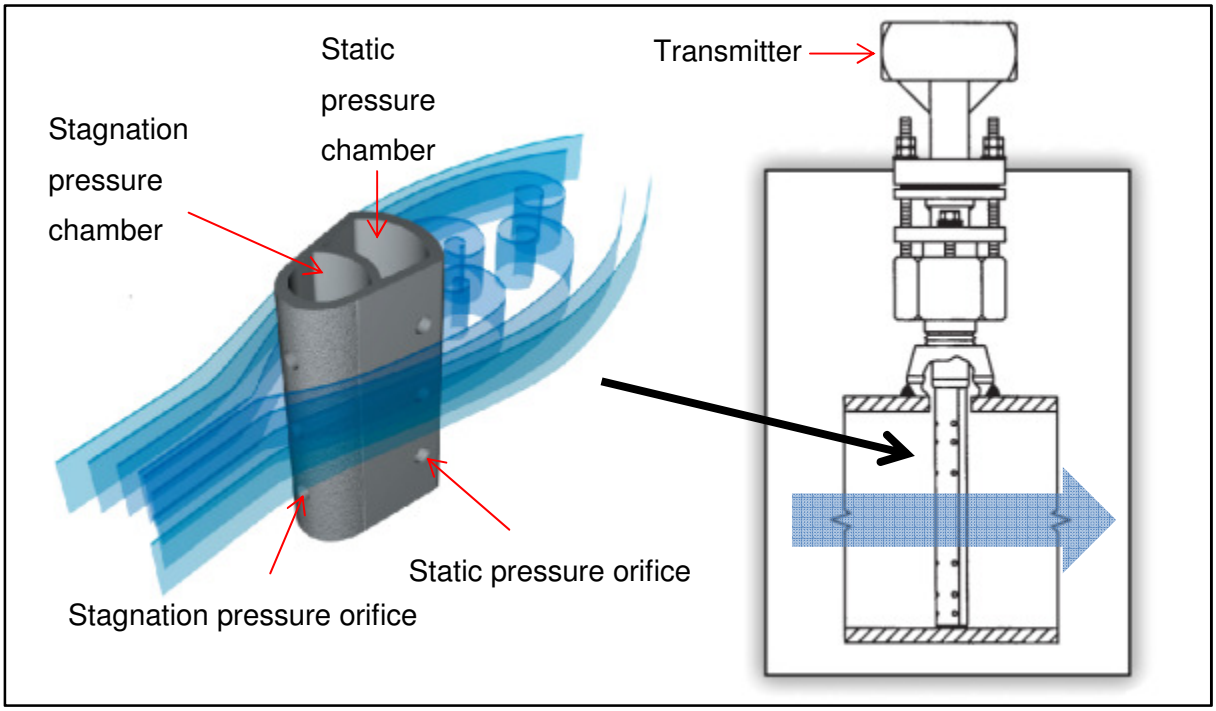

Figure 19: Verabar flow meter by Veris [32]

This flow meter measures the static and stagnation pressure. A pitot static tube uses a similar method to calculate the relative air speed of an aircraft [27, p. 109]. Bernoulli's Equation for frictionless flow for the flow meter reduces to:

$$P_o = P_s + \frac{\rho v^2}{2} \qquad 3.10$$

where P_s is the static pressure; and
P_o is defined as the stagnation pressure.

Solving Equation 3.10 gives the average fluid velocity, v:

$$v = \sqrt{2(P_o - P_s)/\rho} \qquad 3.11$$

The Verabar flow meter uses the average fluid velocity and internal diameter of the pipe to give an output in m^3/h. Equation 3.7 can then be used to calculate the mass flow. The following graph in Figure 20 shows the average shaft mass air flow, measured over a period of one month.

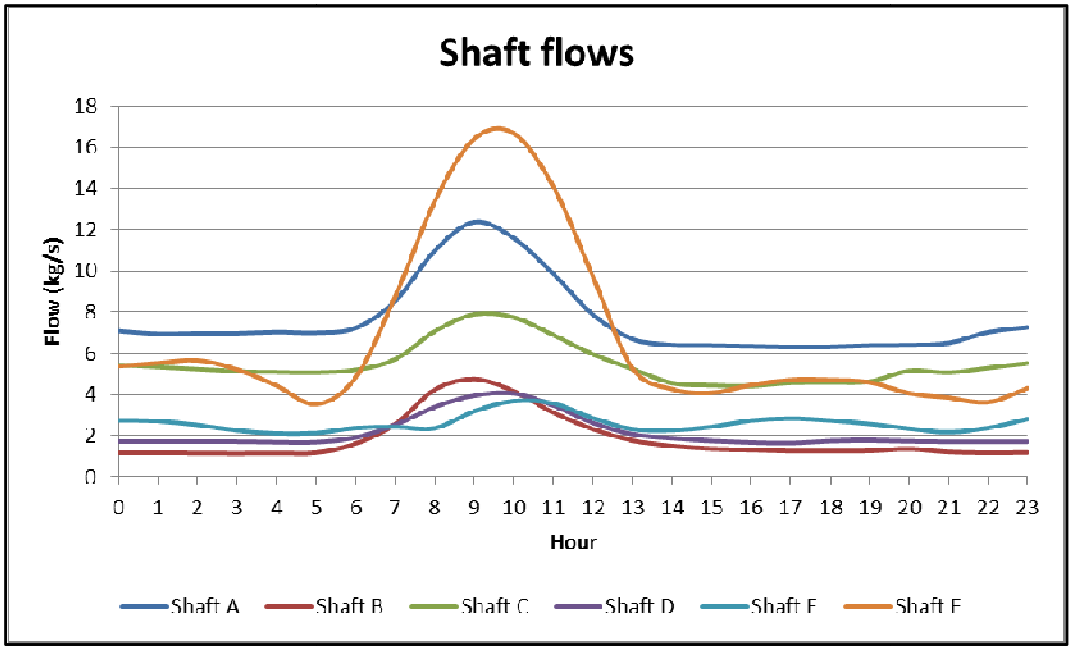

Figure 20: Average shaft mass air flows

3.5 Pipeline properties

The distances between shafts, compressor houses and pipe junctions were measured using Google Earth[5]. By comparing logged GPS coordinates taken at two locations and the locations in Google Earth after giving the logged coordinates as input, it was found that there was an error of 0.32% over a distance of 2 829.72 m.

[5] Google Earth developed by Google, http://www.google.com/earth/.

3.5.1 Air losses

Reducing the pressure of the compressed air network has energy-efficiency benefits [17]. Consider a container that has an orifice and is filled with compressed air representing a pipe section. Assuming that the fluid's initial velocity out of the container is zero and the elevation at the entrance and exit of the orifice is the same, Equation 3.5 can be used to obtain:

$$\Delta P = K_{orifice} \frac{\rho_2 v_2^2}{2} \qquad 3.12$$

where $K_{orifice}$ is the orifice loss factor.

The graph in Figure 21 was obtained using Equation 3.12 with $K_{orifice} = 0.8$. This graph shows the effects of different system pressures on the leaks, expressed in terms of mass air flow through different orifice sizes. Figure 21 clearly shows that the lower the system pressure, the less flow is lost through pipe leaks.

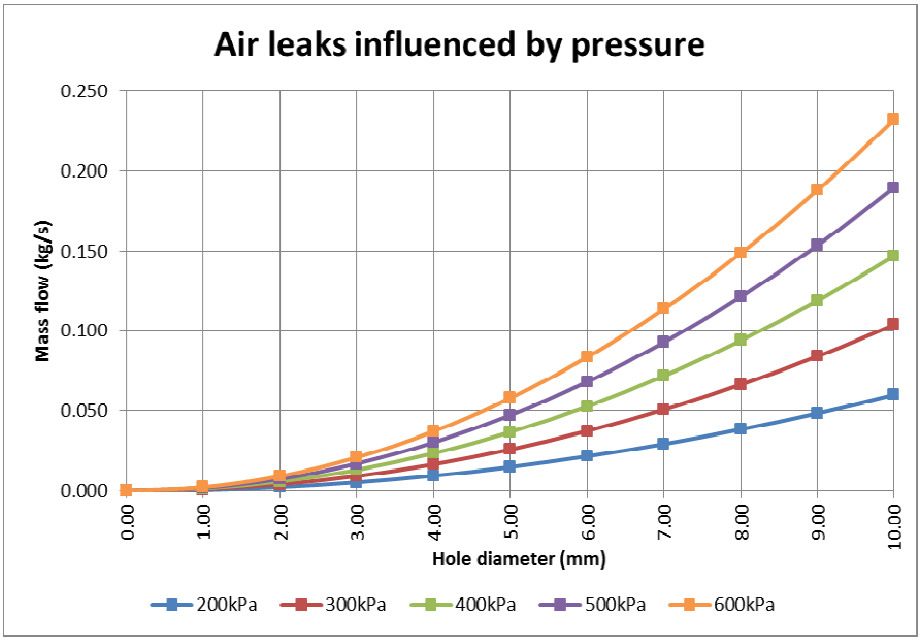

Figure 21: Air leakage at different pressures

Similar properties are valid for pneumatic equipment, shaft ventilation and cooling equipment. The minimum equipment pressures of these compressed air users are specified by the original equipment manufacturer (OEM). Increasing the compressed air pressure will not necessarily result in an increase in equipment performance. A lower system pressure, resulting in reduced flow losses, implies less energy consumption to generate the required system pressure.

3.5.2 Pipe friction pressure losses

Pipe friction losses are a major cause of system pressure losses. The pressure losses as a result of internal pipe wall roughness can be calculated from Equation 3.13 [27, p. 431].

$$\Delta P_{friction} = f \frac{L}{D} \frac{\rho v^2}{2} \tag{3.13}$$

Where f is the friction factor and is given by Equation 3.14 [27, p. 435]:

$$\frac{1}{\sqrt{f}} = -2 * \log\left(\frac{\varepsilon/D}{3.7} + \frac{2.51}{Re\sqrt{f}}\right) \tag{3.14}$$

For equations 3.13 and 3.14:
L is the pipe length;
D is the pipe diameter;
ρ is the fluid density;
v is the fluid velocity; and
ε is the equivalent pipe roughness.

An accuracy of 10% can be expected in pipe flow calculations because of necessary assumptions that have to be made, for example, the pipe roughness [27, p. 435].

The Colebrook Equation is implicit and has to be solved numerically. This over-complicates the computer-aided solving of the friction factor, f. Derived approximation equations are available. Equation 3.15 shows the Swamee and Jain approximation of the Colebrook Equation [33]. For the specific conditions of the mine, this approximation is sufficient.

$$f = {0.25}\Big/{\left[\log\left(\frac{\varepsilon}{3.7D} + \frac{5.74}{Re^{0.9}}\right)\right]^2} \qquad 3.15$$

An estimate for a pipe's equivalent roughness is shown in Table 1. The pipes of the compressed air network are not new, however, and some have deteriorated considerably over many years. An equivalent roughness of 45 µm is assumed for the entire compressed air network. From the simulations done in Chapter 4, this assumption was found to be correct.

	Equivalent Roughness, ε	
Pipe	**Feet**	**Millimeters**
Riveted steel	0.003–0.03	0.9–9.0
Concrete	0.001–0.01	0.3–3.0
Wood stave	0.0006–0.003	0.18–0.9
Cast iron	0.00085	0.26
Galvanized iron	0.0005	0.15
Commercial steel or wrought iron	0.00015	0.045
Drawn tubing	0.000005	0.0015
Plastic, glass	0.0 (smooth)	0.0 (smooth)

Table 1: Equivalent roughness for new pipes [27, p. 433]

3.5.3 Pipe geometry pressure losses

These pipe losses are the result of geometrical changes in the pipe line, such as bends, tees, valves, etc. [27, p. 436]. Using equation 3.12 with a different loss factor, the pressure loss can be calculated.

$$\Delta P = K_{geometry} \frac{\rho_2 v_2^2}{2} \qquad 3.16$$

Table 2 shows typical $K_{geometry}$ values for loss components.

Component	K_L
a. Elbows	
Regular 90°, flanged	0.3
Regular 90°, threaded	1.5
Long radius 90°, flanged	0.2
Long radius 90°, threaded	0.7
Long radius 45°, flanged	0.2
Regular 45°, threaded	0.4
b. 180° return bends	
180° return bend, flanged	0.2
180° return bend, threaded	1.5
c. Tees	
Line flow, flanged	0.2
Line flow, threaded	0.9
Branch flow, flanged	1.0
Branch flow, threaded	2.0
d. Union, threaded	0.08
***e. Valves**	
Globe, fully open	10
Angle, fully open	2
Gate, fully open	0.15
Gate, $\frac{1}{4}$ closed	0.26
Gate, $\frac{1}{2}$ closed	2.1
Gate, $\frac{3}{4}$ closed	17
Swing check, forward flow	2
Swing check, backward flow	∞
Ball valve, fully open	0.05
Ball valve, $\frac{1}{3}$ closed	5.5
Ball valve, $\frac{2}{3}$ closed	210

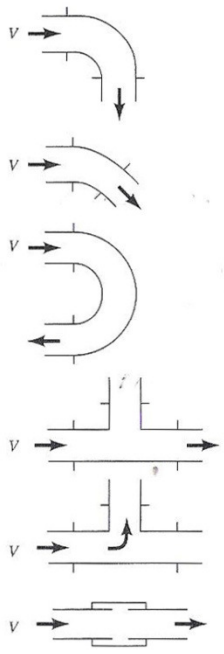

Table 2: Loss coefficients for pipe components [27, p. 445]

However, it is impossible to accurately assign the table values to the various bends, elbows, tees and joints that are found on the mine's compressed air network. The loss factors will therefore be determined once off by using historical system pressures and flows.

Equation 3.13 and 3.16 can be combined to form one equation:

$$\Delta P_{total} = \Delta P_{friction} + \Delta P_{geometry} = \left(f\frac{L}{D} + K_L\right)\frac{\rho v^2}{2} \qquad 3.17$$

Equation 3.17 was used in the DCS solver to account for the combined pressure losses.

3.6 Network solving approaches

It is not practical to measure the pipe lengths that are installed underground and to include them in the simulations[6]. The underground compressed air networks are also often randomly altered by mining staff and it would be too difficult to keep changes up to date. A typical example is where mine workers want additional air for ventilation and create a compressed air bleed-off point. The pressure nodes that will be used for simulations start at the compressor house exit and end at the shaft entrances where the pipeline goes underground.

[6] The combined underground pipe length of one of the shafts is 160 km. These pipes have smaller internal diameters than the surface pipes and range from 250 mm for drilling equipment 250 mm for the main supply lines.

There are two approaches that can be taken to solve the compressed air network, namely an analytical or a numerical approach. Although there are many solving techniques that can be described by these approaches, only the techniques that were considered will be discussed.

The first two methods that are discussed (the electric-hydraulic analogy and the Hardy-Cross Method) are not very user friendly. Even experienced users with a good understanding of how to set up the equations still find these methods cumbersome. They are also susceptible to human error. The aim of developing the DCS is to have a generic network solving tool and compressor selector that can easily be implemented for similar systems.

3.6.1 Electric-hydraulic analogy

An electric-hydraulic analogy can be used to solve a system comprising multiple pipes. The compressed air network can be solved using node-and-loop equations analogous to solving an electric circuit. This is because the same mathematical model can be used to explain two very different physical systems [34, p. 118]. For each node, the net flow needs to be zero so that the law of mass conservation holds true [27, p. 463]. The fluid flow rate is analogous to current (the flow of electrons) and the pressure drop across a pipe section is analogous to a voltage drop across a resistor [35, p. 138]. Table 3 on the following page shows the analogy between an electric and a hydraulic system.

A set of simultaneous equations can be set up and solved using the substitution method.

Property	Electrical element or equation	Hydraulic or fluid analogy
Potential variable	Voltage or potential difference, $v_1 - v_2$	Pressure difference, $P_1 - P_2$
Flow variable	Current flow, i	Fluid volume flow rate, q_f
Resistance	Resistor, R	Fluid resistor, R_f
Capacitance	Capacitor, C	Fluid capacitor, C_f
Inductance	Inductor, L	Fluid inertor, I_f
Power dissipation	$P = i^2 R$	$P_f = q_f^2 R_f$
Potential energy storage	$W_p = \frac{1}{2} C v^2$	$W_p = \frac{1}{2} C_f p^2$
Kinetic energy storage	$W_k = \frac{1}{2} L i^2$	$W_k = \frac{1}{2} I_f q_f^2$

Table 3: Analogy between electrical and fluid circuits [35, p. 140]

3.6.2 Hardy-Cross Method

A similar solving procedure is the Hardy-Cross method. This requires setting up the appropriate flow equations. These equations are solved by assuming suitable initial flow parameters for each loop in the network [33]. With each iteration, the flow through a loop is adjusted until the desired accuracy is achieved [36, p. 216].

3.6.3 Numerical method

For the DCS application, it is easier to use a numerical iterative solving approach. By using this approach, base building blocks can be defined for the system. This will require minimal setup from an end user.

Simplified network calculation

Calculations are shown in Appendix A.

Equation 3.18 is obtained by assuming constant parameter values for Equation 3.17, except for the pressures and fluid flows[7], denoted as B.

$$\Delta P = B * v^2 \qquad 3.18$$

with

$$B = \left(f \frac{L}{D} + K_L\right) \frac{\rho}{2} = \text{constant} \qquad 3.19$$

Consider a simplified compressed air network with all the pipes having the same properties, as shown in Figure 22.

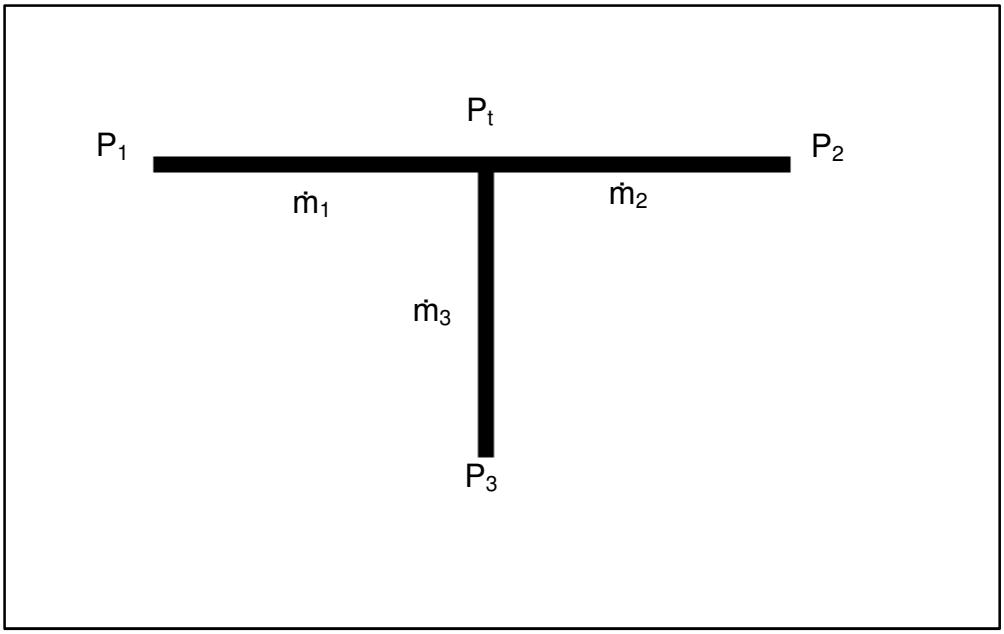

Figure 22: Simple network layout

[7] The Colebrook friction factors for major pipe losses and fluid densities do not remain constant and will have to be calculated for each pipe's fluid flow for the DCS.

P_1 represents a source of compressed air, namely a compressor house. P_2 and P_3 represent compressed air consumers, namely shafts. P_t is the intermediate node pressure. From equations 3.8 and 3.18, the following set of equations is obtained that describes the system:

$$\begin{aligned} P_1 - P_t &= B * v_1^2 \\ P_t - P_2 &= B * v_2^2 \\ P_t - P_3 &= B * v_3^2 \\ \dot{m}_1 &= \dot{m}_2 + \dot{m}_3 \end{aligned} \qquad 3.20$$

where v_x is the fluid velocity; and
$\dot{m}_x$ is the air mass flow

To solve the network shown in Figure 22, each pipe is considered separately during each iteration. Figure 23 illustrates this.

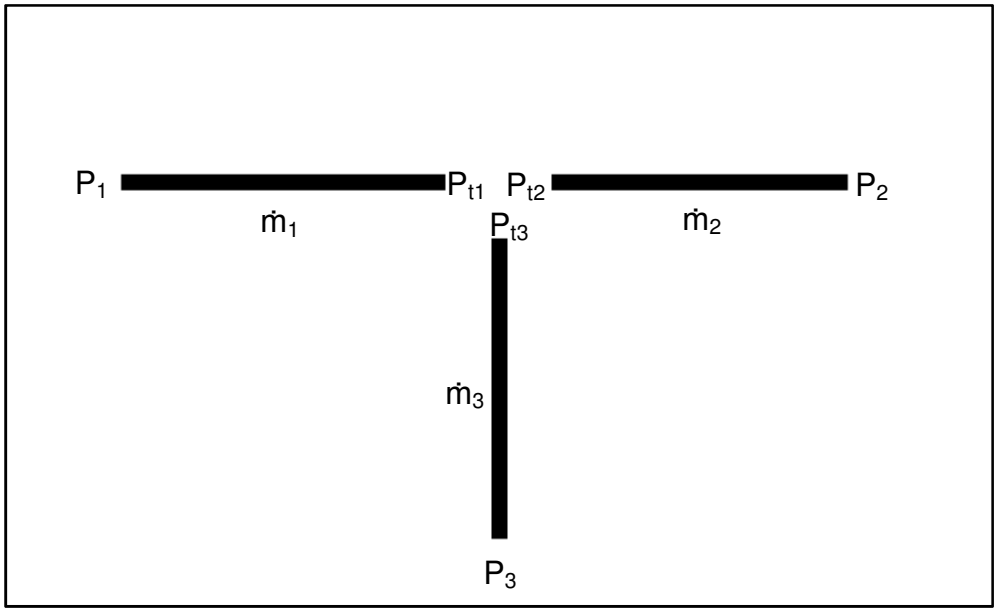

Figure 23: Simple network layout solving logic

Initial values for the flows are chosen arbitrarily. The intermediate pressure of each equation, shown in Equation 3.21, can now be calculated.

$$\begin{aligned} P_1 - P_{t1} &= B * v_1^2 \\ P_{t2} - P_2 &= B * v_2^2 \\ P_{t3} - P_3 &= B * v_3^2 \\ \dot{m}_1 &= \dot{m}_2 + \dot{m}_3 \end{aligned} \qquad 3.21$$

The intermediate pressures, P_{t1}, P_{t2} and P_{t3}, represent the same pressure at the common node and are calculated using the initial flow assumptions. If the calculated pressure values differ by more than 0.1 Pa, then the average value of these pressure differences will be used for a new iteration. This average pressure is then used to calculate new mass flow values.

If the two sides of the conservation of mass equation differ by more than 0.1 kg/s, the right-hand side is used to calculate a new intermediate pressure. The process is repeated until the intermediate pressure difference is within 0.1 Pa.

The intermediate pressure can also be varied between the maximum pressure (P_1) and the minimum pressure (P_1 or P_2) until the conservation of mass is within acceptable limits:

$$\dot{m}_1 \approx \dot{m}_2 + \dot{m}_3 \qquad 3.22$$

This makes the solving technique independent of convergence and will be used for the DCS solving technique.

The DCS solving technique

This technique ensures that the intermediate node pressure is always less than the maximum upstream pressure and greater than the minimum downstream pressure. Each node is evaluated separately, with initial values given to the unknown adjacent points and replaced with updated values after each iteration. The appropriate equations for pipe and fluid properties are used to solve the conditions of all the pipes during every iteration.

Figure 24 shows a simple layout consisting of two shafts, a compressor house and one intermediate node. The node flows are represented by $N_x(y)$, where x is the node number and y is the pipe number. The intermediate node pressure is represented by $N_x(0)$.

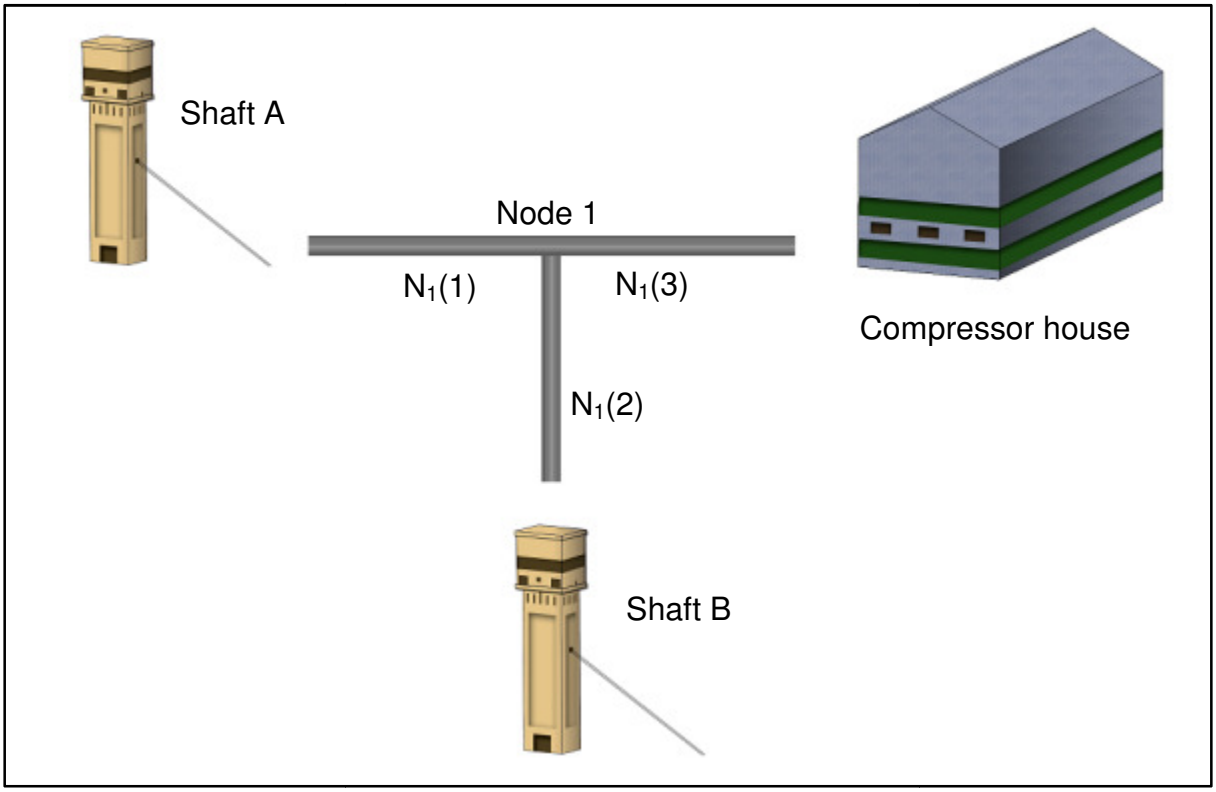

Figure 24: One-node layout

The pressure(s) at the point(s) of compressed air production and consumption (Shaft A, Shaft B and the compressor house) are known variables. When the DCS is implemented, these pressures will continuously be monitored using permanently installed pressure transmitters. The pressures will be used to solve the compressed air network for various system parameters.

As an iterative starting point for the pressure at Node 1, the average pressures of the three known points are used. The pressure of Node 1 is then varied until the continuity equation of mass, Equation 3.23, is satisfied. This will give the node pressure and the flows in the three pipes.

$$N_1(1) - N_1(2) - N_1(3) \approx 0 \qquad 3.23$$

Figure 24 shows a more complex layout consisting of three shafts, a compressor house and two intermediate nodes.

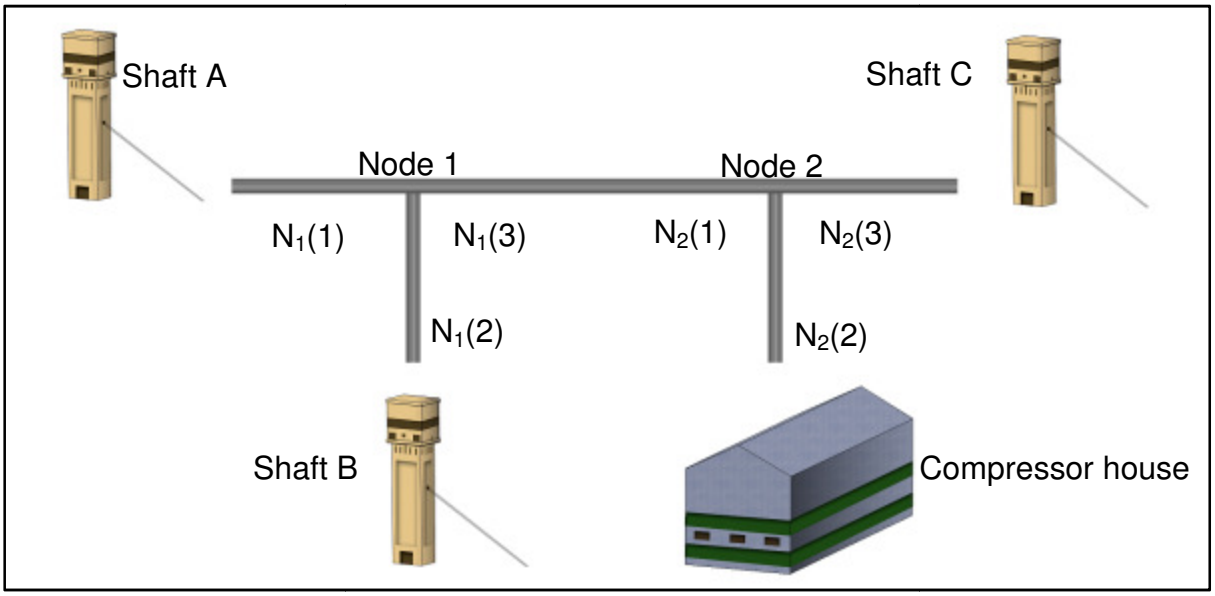

Figure 25: Two-node layout

For this setup, the individual intermediate nodes are considered separately. As an iterative starting point for the pressure at Node 1, the average pressure of the three surrounding points is used. As the pressure of Node 2 is not yet known, the average pressure of all the known points are initially used (that is the pressure of Shaft A, Shaft B, Shaft C and that of the compressor house).

The pressure of Node 1 is then varied until the continuity of mass equation, Equation 3.23, is satisfied. Node 1's pressure has also been solved in the process. For the calculation of Node 2's pressure, the pressure value of the first iteration of Node 1 is used. Node 1 (first iteration), Shaft C and the compressor house's pressure is used to calculate the first iteration's Node 2 pressure value by varying it until the continuity of mass flow is satisfied.

$$\mathrm{N}_2(1) - \mathrm{N}_2(2) - \mathrm{N}_2(3) \approx 0 \qquad 3.24$$

This process is then repeated using the previous iteration's values until $N_1(3) \approx N_2(1)$. Note that $N_1(3)$ and $N_2(1)$ represent the same mass flow through the same pipe section (See Figure 25).

This method avoids values that are higher than the maximum upstream pressure and lower than the minimum downstream pressure and will always converge toward a solution.

3.7 Compressor mapping

The mine does not have compressor performance maps of the installed compressors. Sufficient historical compressor data was available, however. The data includes guide vane angle, blow-off valve position, compressor stage temperature and pressure, outlet and inlet flow, temperature and pressure. Power consumed by the compressor motor was also recorded from the specially connected and installed watt meters. Graphs for the compressors were compiled from the historical data.

Figure 26, Figure 27 and Figure 28 on show the performance characteristics of a VK40. These graphs were constructed using the historical data with the compressor operating and the blow off valve closed. When the blow off valve is open, the air flow cannot be measured accurately.

Various efficiencies have been defined for a compressor, including volumetric, mechanical and hydraulic. For this study, thermo-efficiency was used. Compressor efficiency is defined by Equation 3.25 and can be seen in Figure 28 [8, p. 185], [6, p. 10].

$$\eta_c = \frac{\text{Ideal power}}{\text{Actual power}} \qquad 3.25$$

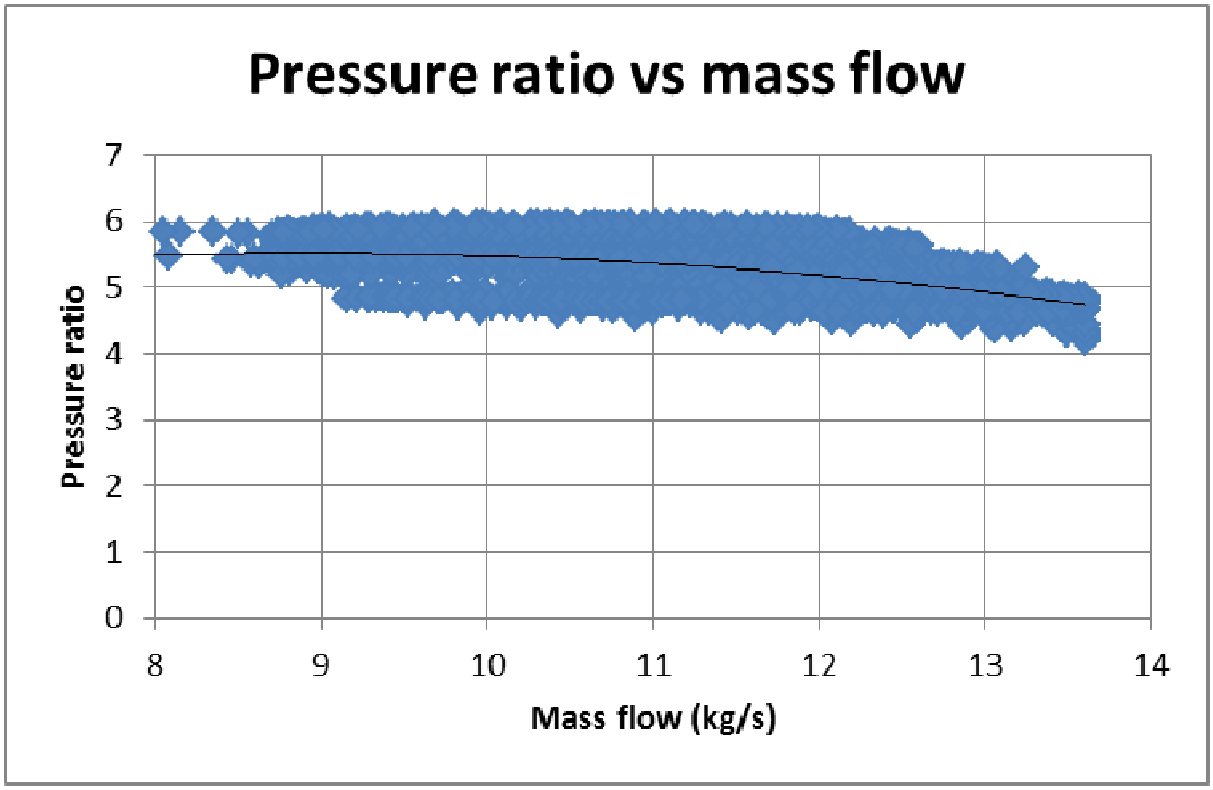

Figure 26: Pressure ratio performance characteristic curve

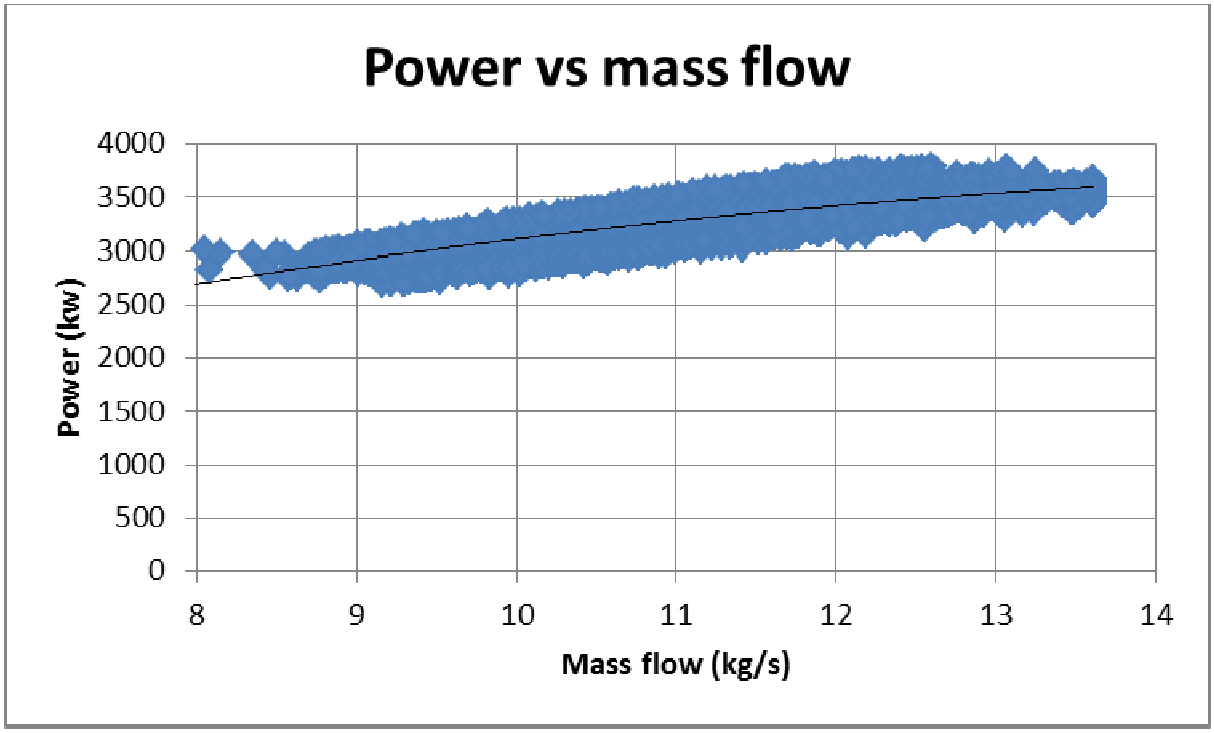

Figure 27: Power performance characteristic curve

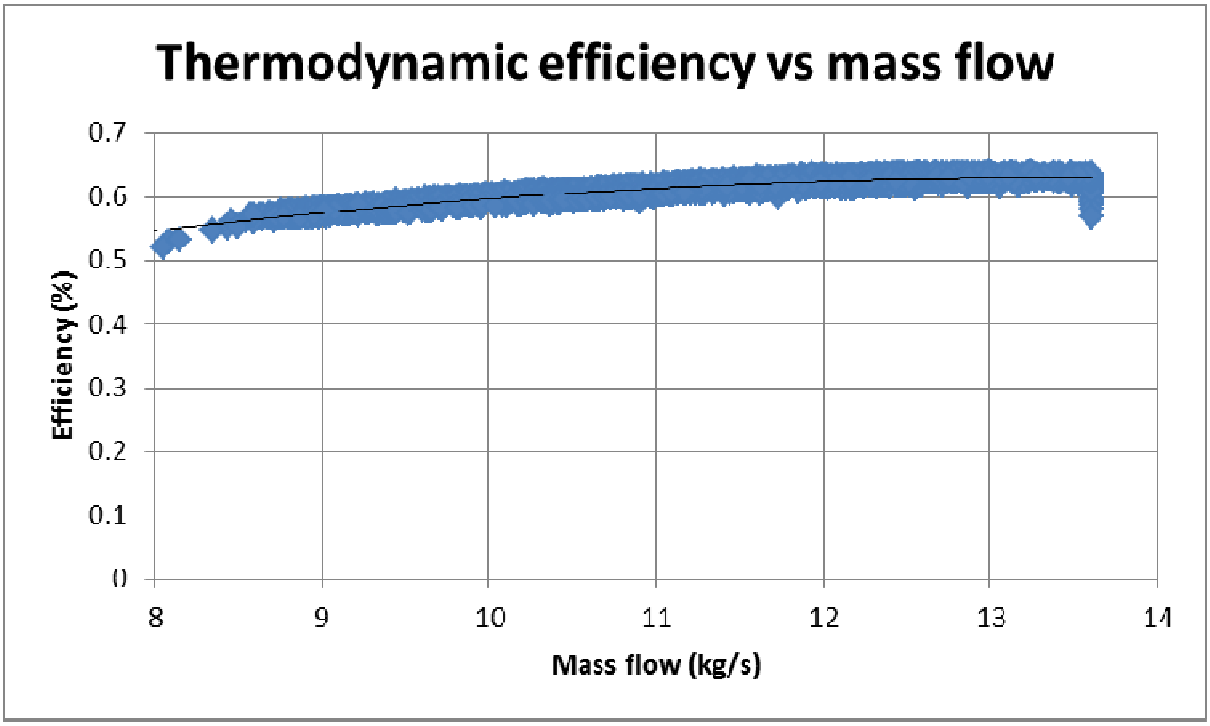

Figure 28: Efficiency characteristic curve

The large amount of data in Figure 26, Figure 27 and Figure 28, which was used make the individual data points indistinguishable, resulted in the dark blue data distribution shown in each figure. The black line is the trend line of the data distribution in each graph. These trend lines were used to compile performance characteristics for the various compressors on the mine.

Note that the compressors of the mine have a fixed rotational shaft speed. Variable speed drive (VSD) technology can be used to vary the rotation speed of the compressor motor [37, p. 543]. Significant energy savings opportunities are possible by using VSDs [37, p. 549]. However this technology is relatively expensive and was not considered for this study [37, p. 548].

Compressor selection philosophy

Simulating the compressed air network is a useful tool to determine which compressors are required to achieve the most efficient air delivery. However, costs associated with starting and/or stopping a compressor and maintenance costs must also be considered [2, p. 178], [15, p. 36], [16, p. 13]. Maintenance schedules and cost details were not available from the mine. For this reason, historical data was used to determine how frequently and at what time intervals a compressor was started and stopped.

Compressors belonging to the same compressor house deliver the same set point pressure and supply a common manifold. This means that air flow requirements for a given set point pressure will determine how many compressors are required. The demands of the shafts vary constantly. However, it is not desirable for compressors to be stopped and started whenever this demand changes. An intelligent compressor selection method must be used to prevent compressor cycling.

When the air flow requirement has been determined by the network solver, the compressor selector assesses each compressor, based on logged historical data. The selector will calculate the least amount of compressors required to satisfy system demand. The compressor that can deliver the most flow without exceeding

the required flow will be the first compressor to be selected. If the air flow is still insufficient, the next largest compressor will be selected. This ensures that these compressors operate at fully open guide vane angles, and therefore maximum efficiency.

The last compressor that will be selected will preferably be based on its flow at a 50% guide vane opening. This will ensure that for relatively small changes in demand, compressor blow-off and cycling will not occur. Small changes in flow demand will be met by adjusting the variable guide vanes of the last compressor.

Figure 29 shows the guide vane angle of a VK40 as a function of mass flow.

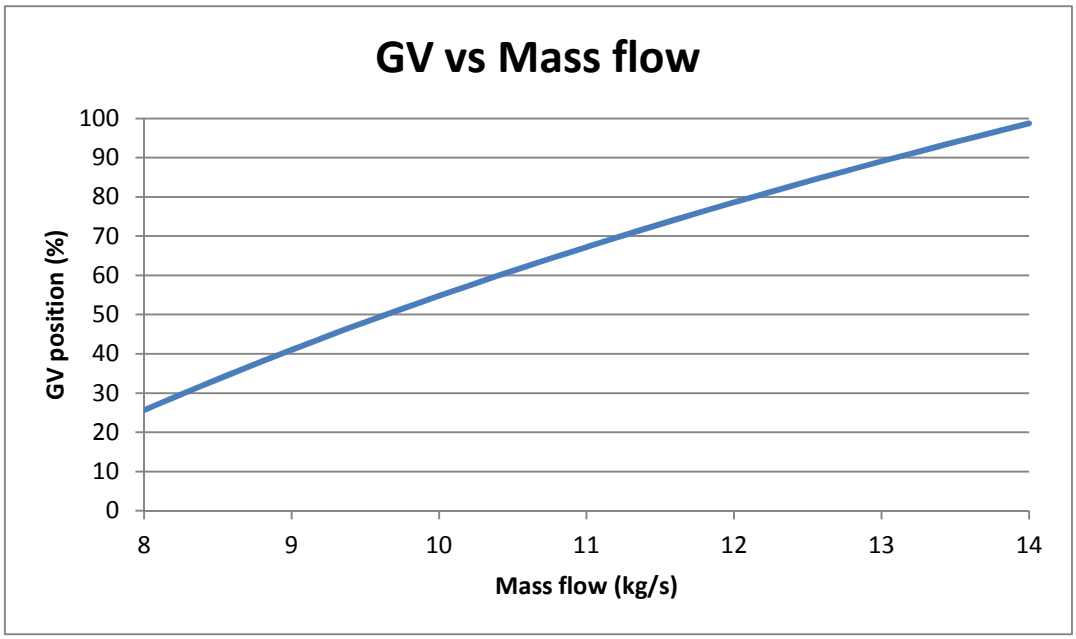

Figure 29: Guide vane angle vs mass flow

The following example will illustrate this selection process.

Assume that the flow required from a compressor house is 25 kg/s and that the following compressors are available:

	Flow range (kg/s)
Compressor 1	7 to 9
Compressor 2	9 to 11
Compressor 3	2 to 3
Compressor 4	2.5 to 3.5
Compressor 5	9 to 11

Table 4: Compressor flow ranges

The compressor selector will select Compressor 2 and Compressor 5 based on their maximum flows. However, an additional 3 kg/s mass flow is still required. Because the mass flow of any remaining compressor will be sufficient to provide the extra 3 kg/s, the compressor selector will not select Compressor 3. Instead, Compressor 4 will be selected so that there is a safety margin for a relatively small change in demand.

3.8 The DCS solution

The DCS consists of two distinct elements, namely network solving and compressor control. These two elements are discussed, followed by a brief discussion regarding the risks in the case of a network communication failure.

3.8.1 Network solving

The chart on the following page illustrates the network solving process.

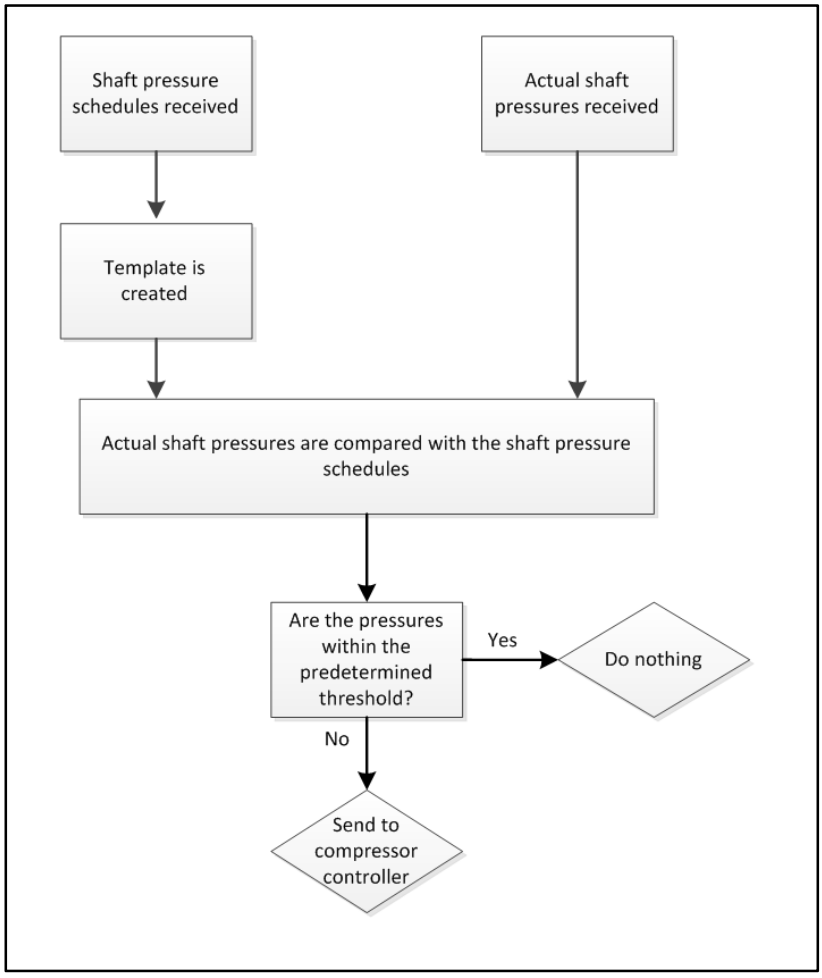

Figure 30: Simplified flow chart illustrating the network solving process

Each shaft has a surface control valve setup with a predetermined pressure schedule. This schedule is updated by the shafts' instrumentation personnel according to the daily production schedule. The pressure schedules of all the shafts are used to compile a template against which the actual pressures will be compared. Pressure and flow values at each compressor house are measured to ensure that the end user pressure and flow requirements are maintained.

3.8.2 Compressor control

The following chart illustrates the compressor selection process:

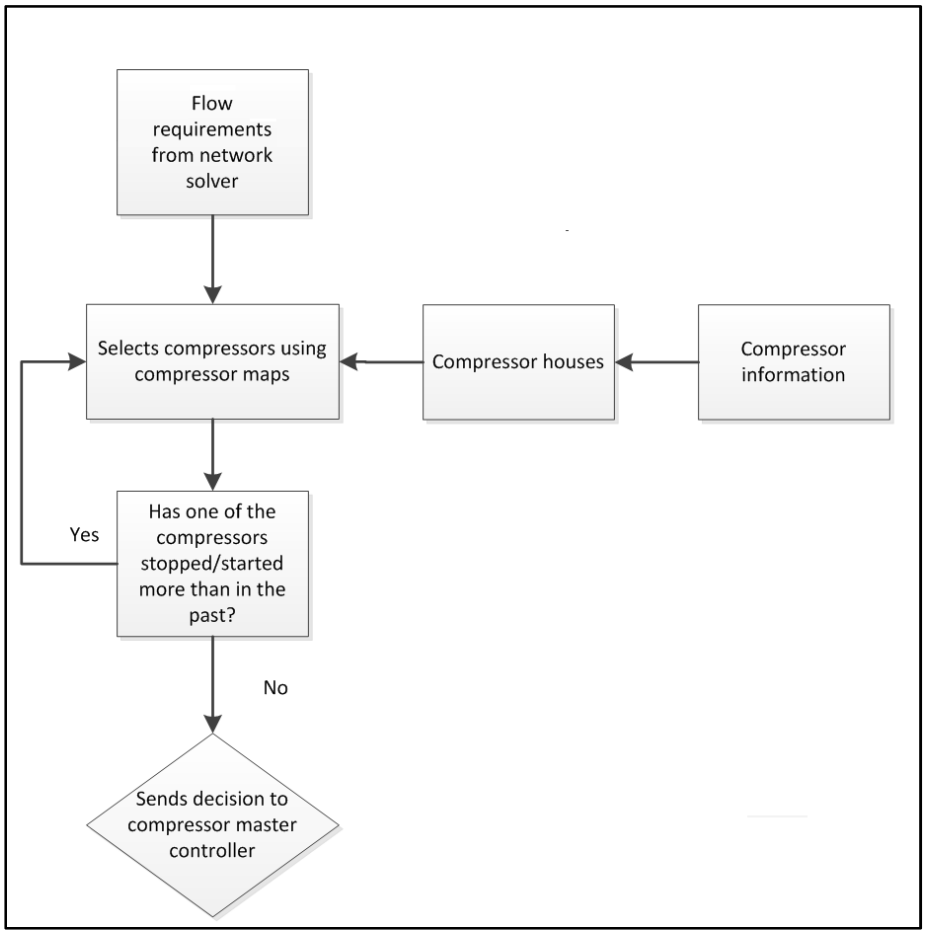

Figure 31: Simplified flow chart illustrating the compressor selection process

When the pressure requirements of one or more shafts exceed the predetermined pressure limitations, the compressor controller will send commands to adjust these parameters. Air flow and pressures calculated by the network solver will determine which compressors must be used to obtain the results dictated by the network template. A simple pressure set point offset will be given to the lowest priority compressor to ensure that this compressor alone adjusts the system pressure.

3.8.3 Compressor control room operator

With the implementation of DCS, the control room operator does not have to adjust the compressor priorities or pressure set points. The control room operator will be tasked with keeping the fixed compressor priority list of the present master controller updated in case of a network communication failure. The system will revert back to the present master controller's control philosophy if this happens.

3.8.4 Network communication

DCS will dynamically change the compressor priorities and pressure set points on the present compressor master controller. In the case of a network communication failure, the present compressor master controller will revert back to a fixed compressor priority list, as mentioned in section 3.8.3. Therefore, the compressor control will be just as safe as before the implementation of DCS.

3.8.5 Quantifying pressure loss components

An assumption regarding the pipe roughness is made. The pipe geometry pressure losses have to be determined empirically for the compressed air network.

3.9 Conclusion

Assumptions pertaining to fluid flow, pipes of the compressed air network and compressor performance were made to simplify the development of DCS. The assumptions are within the 10% accuracy range that can be expected from pipe flow calculations. Compressed air properties, pipeline properties, network-solving approaches, compressor mapping and a compressor selection were investigated. This led to a DCS solution that is verified with theoretical and actual logged historical data in Chapter 4.